1521-0103/345/1/139–150$25.00
THE JOURNAL OF PHARMACOLOGY AND EXPERIMENTAL THERAPEUTICS

http://dx.doi.org/10.1124/jpet.112.201566
J Pharmacol Exp Ther 345:139–150, April 2013

Group I mGluRs Evoke K-ATP Current by Intracellular Ca^{2+} Mobilization in Rat Subthalamus Neurons

Ke-Zhong Shen and Steven W. Johnson

Department of Neurology, Oregon Health & Science University, Portland, Oregon (K.-Z.S., S.W.J.); and the Portland Veterans Affairs Medical Center, Portland, Oregon (S.W.J.)

Received November 1, 2012; accepted January 17, 2013

ABSTRACT

We reported previously that Ca^{2+} influx through *N*-methly-D-aspartate-gated channels evokes ATP-sensitive K^+ (K-ATP) currents in rat subthalamic nucleus (STN) neurons. By using whole-cell patch clamp recordings in brain slices, we investigated the ability of (*RS*)-3,5-dihydroxyphenylglycine (DHPG), a group I metabotropic glutamate receptor (mGluR) agonist, to evoke K-ATP currents. DHPG (20 μM) evoked outward current at −70 mV and was associated with a positive slope conductance of 2.7 nS. The sulfonylurea agent tolbutamide (100 μM) converted the positive slope to negative slope conductance, indicating mediation by K-ATP channels (ATP-sensitive K+ channels). Currents evoked by DHPG were significantly reduced by a combination of mGluR1 and mGluR5 negative allosteric modulators. DHPG-evoked outward current was blocked by cyclopiazonic acid and thapsigargin and mimicked by caffeine, suggesting mediation by release of intracellular Ca^{2+}. DHPG outward current was also blocked by ryanodine and 2-aminoethoxydiphenylborane, suggesting mediation by ryanodine- and inositol 1,4,5-triphosphate-sensitive Ca^{2+} release. The nitric oxide synthase inhibitor N^G-nitro-L-arginine methyl ester and inhibitors of protein kinase G activity also suppressed DHPG-induced outward current. Voltage recordings showed that tolbutamide prolonged depolarizing plateau potentials and increased the spontaneous firing rate of STN neurons recorded in the presence of DHPG. These results show that group I mGluR stimulation generates K-ATP current by a nitric oxide- and protein kinase G-dependent process that is mediated by release of Ca^{2+} from intracellular stores. Because burst firing is linked to symptoms of Parkinson's disease, we suggest that K-ATP channels might provide a physiologically important inhibitory influence on STN neuronal activity.

Introduction

The subthalamic nucleus (STN) is composed of glutamate-containing neurons that project to the principal output nuclei of the basal ganglia: the substantia nigra pars reticulata (SNR) and globus pallidus interna (Féger et al., 1997). Because the STN regulates outflow from the basal ganglia, the STN plays a pivotal role in regulating normal and abnormal movement (Albin et al., 1995). For example, loss of dopaminergic innervation of the basal ganglia increases burst firing in the STN and basal ganglia output nuclei, and this correlates with many of the cardinal features of Parkinson's disease (Bergman et al., 1994). Moreover, high-frequency stimulation of the STN has been shown to reduce burst discharges in STN and SNR neurons in animal models of Parkinson's disease (Breit et al., 2007; Maltete et al., 2007). Regularization of STN output is believed to provide the basis for the effectiveness of deep brain stimulation in the treatment of Parkinson's disease (Maltete et al., 2007; Xu et al., 2008). On the other hand, silencing STN output, either by lesion or chemically induced inhibition, evokes hyperkinetic movements such as ballism and chorea in monkeys, rats, and humans (Guridi et al., 1996; Chen et al., 2002; Mehta et al., 2005). These results suggest that abnormally reduced output from STN neurons induces hyperkinetic movements, whereas irregular burst discharges contribute to the rigidity and bradykinesia seen in Parkinson's disease.

Because the STN plays such an important role in movement, it is important to understand how output from the STN is regulated by synaptic inputs and pharmacological agents. The STN receives glutamate-containing inputs from cerebral

This work was supported by the National Institutes of Health National Institute of Neurological Disorders and Stroke [Grant NS38715]; and by the Portland Veterans Affairs Parkinson's Disease Research, Education, and Clinical Center.
dx.doi.org/10.1124/jpet.112.201566.

ABBREVIATIONS: ANOVA with RM, analysis of variance with repeated measures; AP5, 2-amino-5-phosphonopentanoic acid; 2-APB, 2-aminoethoxydiphenylborane; CPCCOEt, 7-(hydroxyimino)cyclopro-pa[*b*]chromen-1a-carboxylate ethyl ester; DHPG, (*RS*)-3,5-dihydroxyphenylglycine; InsP3, inositol 1,4,5-trisphosphate; I-V plot, current-voltage plot; JNJ16259685, (3,4-dihydro-2*H*-pyrano[2,3-*b*]quinolin-7-yl)-(*cis*-4-methoxycyclohexyl)-methanone; K-ATP channel, ATP-sensitive K+ channel; L-NAME, N^G-nitro-L-arginine methyl ester hydrochloride; LY83583, 6-anilino-5,8-quinolinedione; mGluR, metabotropic glutamate receptor; MPEP, 2-methyl-6-(phenylethynyl)pyridine HCl; MTEP, 3-[(2-methyl-1,3-thiazol-4-yl)ethynyl]-pyridine; NMDA, *N*-methly-D-aspartate; NO, nitric oxide; NOS, nitric oxide synthase; ODQ, 1*H*-[1,2,4]oxadiazolo[4,3-a]quinoxalin-1-one; PKG, cGMP-dependent protein kinase; Rp-8-Br-PET-cGMPs, 2-bromo-3,4-dihydro-3-[3,5-*O*-[(*R*)-mercaptophosphinylidene]-β-D-ribofuranosyl]-6-phenyl-9*H*-imidazo[1,2-*a*]purin-9-one sodium salt; SNC, substantia nigra pars compacta; SNR, substantia nigra pars reticulata; STN, subthalamic nucleus.

cortex, thalamus, and pedunculopontine nucleus, whereas a large GABA input arises from the globus pallidus externa (Canteras et al., 1990; Féger et al., 1997). Although glutamate is the principal excitatory transmitter in the STN, the net effect of glutamate will depend upon the receptor subtype being activated and subsequent involvement of second messenger systems. For example, our laboratory recently reported that stimulation of the *N*-methyl-D-aspartate (NMDA) subtype of glutamate receptors evoked an inhibitory ATP-sensitive K^+ (K-ATP) current in STN neurons but not in adjacent dopamine neurons in the substantia nigra pars compacta (SNC) (Shen and Johnson, 2010). Our data suggested that Ca^{2+} influx through NMDA-gated channels activated K-ATP channels (ATP-sensitive K+ channels) via nitric oxide- and cGMP-dependent pathways. Moreover, our studies showed that K-ATP channel activation by NMDA shortened depolarizing plateau potentials and reduced burst firing in STN neurons. Thus, coactivation of K-ATP currents has the ability to temper the excitatory influence of NMDA receptor stimulation in the STN.

Similar to NMDA receptors, group I metabotropic glutamate receptors (mGluRs) also elevate intracellular levels of Ca^{2+}. But rather than causing Ca^{2+} influx, group I mGluRs release Ca^{2+} from inositol 1,4,5-triphosphate ($InsP_3$)- and ryanodine-sensitive intracellular Ca^{2+} stores (Fagni et al., 2000). Group I mGluRs, which include the mGluR1 and mGluR5 subtypes, also evoke Ca^{2+}-activated currents in many central neurons (Congar et al., 1997; Tempia et al., 2001). Furthermore, the STN is known to express both mGluR1 and mGluR5 (Wang et al., 2000; Kuwajima et al., 2004, 2007). Moreover, Awad et al. (2000) showed that mGluR5 stimulation evokes an excitatory inward current caused primarily by reducing a resting K^+ conductance in STN neurons in the rat brain slice. The present studies were undertaken to test whether group I mGluR stimulation could also evoke Ca^{2+}-dependent K-ATP current in STN neurons.

Materials and Methods

Tissue Preparation. All procedures were carried out in accordance with a protocol approved by Institutional Animal Care and Use Committee at the Portland Veterans Affairs Medical Center. Every precaution was taken to minimize animal stress and the number of animals used. Horizontal slices containing diencephalon and rostral midbrain were prepared from male Sprague-Dawley rats (Harlan, Indianapolis, IN) as described previously (Shen and Johnson, 2000). Adult rats (120–180 g) were used for STN and SNC recordings; because SNR neurons are difficult to record from adult tissue, SNR neurons were recorded in tissue from young rats (11–26 days old). Briefly, rats were anesthetized with isoflurane and killed by severing major thoracic vessels. Brains were rapidly removed, and slices were cut with a vibratome in an ice-cold sucrose buffer solution of the following composition (in mM): sucrose, 196; KCl, 2.5; $MgCl_2$, 3.5; $CaCl_2$, 0.5; NaH_2PO_4, 1.2; glucose, 20; and $NaHCO_3$, 26, equilibrated with 95% O_2–5% CO_2. A slice containing the STN and substantia nigra was then placed on a supporting net and submerged in a continuously flowing solution (2 ml/min) of the following composition (in mM): NaCl, 126; KCl, 2.5; $CaCl_2$, 2.4; $MgCl_2$, 1.2; NaH_2PO_4, 1.2; $NaHCO_3$, 19; glucose, 11, gassed with 95% O_2 and 5% CO_2 (pH 7.4) at 36°C. By using a microscope for visual guidance, the STN was located as gray matter approximately 2.7 mm lateral to the midline and 2 mm rostral to the center of the SNR.

Electrophysiological Recordings. Whole-cell recordings were made with pipettes containing (in mM): potassium gluconate, 138; $MgCl_2$, 2; $CaCl_2$, 1; EGTA, 0.2; HEPES, 10; ATP, 1.5; GTP, 0.3 (pH 7.3). Pipette resistance ranged from 3 to 8 MΩ, whereas series resistance typically ranged from 15 to 40 MΩ. Membrane currents were recorded under voltage clamp and amplified with an Axopatch-1D amplifier (5-kHz low-pass filter). Baseline holding potentials were −70 mV in STN and SNR neurons and −60 mV in SNC neurons so that holding currents were close to zero. In some experiments, we used a "loose-patch" method to record extracellular currents and potentials (Nunemaker et al., 2003). For loose-patch recordings, patch pipettes were filled with standard extracellular solution; loose-patch recordings were made with a seal resistance typically 5–10 times the starting value of electrode resistance (3–8 MΩ). Data were acquired using a personal computer with a Digidata analog/digital interface and analyzed using pCLAMP software (Molecular Devices/Axon Instruments, Foster City, CA). Currents and potentials were recorded continuously using a MacLab analog/digital interface, Chart software (AD Instruments, Castle Hill, NSW, Australia), and a Macintosh computer. Membrane potentials for whole-cell recordings have been corrected for the liquid junction potential (10 mV).

Current-Voltage Studies. Current-voltage (I-V) relationships were constructed by measuring currents during a series of hyperpolarizing voltage steps (400-millisecond duration) with 10-mV increments from a holding potential of −70 mV (or from −60 mV for SNC neurons). Currents were measured immediately after capacitive transients to minimize the influence of hyperpolarization-activated cation currents. Slope conductance was calculated for each cell as the slope of a straight line in the I-V (current-voltage) plot at voltages between −70 and −100 mV (or between −60 to −90 mV for SNC neurons). Mean slope conductance and S.E.M. were obtained by averaging slope conductances from all cells. In some figures, I-V plots were displayed as "subtracted" currents in which currents recorded during the experimental treatment had been subtracted from those currents recorded in the control condition. Therefore, these subtracted currents represent "net" currents that were produced or blocked by an experimental treatment.

Drugs and Chemicals. All drugs were dissolved in aqueous or dimethyl sulfoxide stock solutions. Most drugs were added to the slice perfusate. Stock solutions were diluted at least 1:1000 to the desired concentration in superfusate immediately prior to use. Approximately 30 seconds were required for the drug solution to enter the recording chamber; this delay was due to passage of the superfusate through a heat exchanger. In some experiments, drugs were added to the internal pipette solution and delivered by passive intracellular dialysis. (*RS*)-3,5-dihydroxyphenylglycine (DHPG), 1*H*-[1,2,4]oxadiazolo[4,3-a]quinoxalin-1-one (ODQ), ryanodine, thapsigargin, 2-aminoethoxydiphenylborane (2-APB), 2-bromo-3,4-dihydro-3-[3,5-*O*-[(*R*)-mercaptophosphinylidene]-β-D-ribofuranosyl]-6-phenyl-9*H*-Imidazo[1,2-*a*]purin-9-one sodium salt (Rp-8-Br-PET-cGMPs), 2-methyl-6-(phenylethynyl)pyridine HCl (MPEP), 3-[(2-methyl-1,3-thiazol-4-yl)ethynyl]-pyridine (MTEP), (3,4-dihydro-2*H*-pyrano[2,3-*b*]quinolin-7-yl)-(*cis*-4-methoxycyclohexyl)-methanone (JNJ16259685), 7-(hydroxyimino)cyclopro-pa[*b*]chromen-1a-carboxylate ethyl ester (CPCCOEt), cyclopiazonic acid, diazoxide, and glibenclamide were obtained from Tocris Cookson Inc. (Ellisville, MO). Apamin, 2-amino-5-phosphonopentanoic acid (AP5), 6-anilino-5,8-quinolinedione (LY83583), caffeine, N^G-nitro-L-arginine methyl ester hydrochloride (L-NAME), and tolbutamide were obtained from Sigma-Aldrich (St. Louis, MO).

Data Analysis. Numerical data in the text and error bars in figures are expressed as mean ± S.E.M. Whenever possible, differences in I-V plots were analyzed using two-way analysis of variance (ANOVA) with repeated measures (RM) followed by the Holm-Sidak pairwise comparison test (SigmaStat; Jandel Scientific, San Rafael, CA). Otherwise, data were analyzed with paired or unpaired *t* tests. Slope conductance and reversal potentials were calculated by linear regression of the I-V relationship for each cell; mean values and S.E.M. were calculated by averaging the results from all cells in each experimental group.

Results

DHPG Increases Membrane Conductance in STN Neurons. We recently reported that Ca^{2+} influx through NMDA receptor-gated channels evokes K-ATP current via a nitric oxide (NO)- and cGMP-dependent process in STN neurons (Shen and Johnson, 2010). Group I mGluRs also raise cellular levels of Ca^{2+}, although this is accomplished by release of Ca^{2+} from intracellular stores rather than from Ca^{2+} influx from the extracellular milieu (Fagni et al., 2000). Moreover, STN neurons are known to express both the mGluR1 and mGluR5 subtypes of group I mGluR (Awad et al., 2000; Kuwajima et al., 2007). Therefore, we were interested to find whether mGluR stimulation could also evoke K-ATP currents in STN neurons. By using the selective group I mGluR agonist DHPG, we first characterized the voltage-dependent effects of DHPG on whole-cell membrane currents recorded from STN neurons and adjacent neurons in the SNR and SNC. As shown in the current traces in Fig. 1A, 20 μM DHPG evoked inward currents in an SNR neuron and in a presumed dopamine neuron in the SNC. However, the same concentration of DHPG evoked an outward current in the STN neuron. On average, DHPG (20 μM) evoked 82 $\pm$ 16 pA of inward current in SNR neurons at -70 mV ($n = 10$) and 86 $\pm$ 17 pA of inward current in SNC neurons at -60 mV ($n = 5$). In contrast, DHPG evoked 41 $\pm$ 7 pA of outward current in STN cells as measured at -70 mV ($n = 26$). To investigate the voltage-dependence of DHPG-evoked currents, we recorded currents during a series of hyperpolarizing voltage steps, as shown in Fig. 1B. The voltage-dependence of whole-cell currents recorded before (control) and during DHPG (20 μM) are shown in Fig. 1C. DHPG caused a significant alteration in the current-voltage (I-V) plot ($n = 25$; $F_{1,7} = 49.96$, $P < 0.01$, two-way ANOVA with RM). I-V plots in Fig. 1D show "net" (subtracted) currents evoked by DHPG in STN, SNC, and SNR neurons. DHPG currents in STN neurons were associated with a positive slope conductance of 2.7 $\pm$ 0.3 nS ($n = 26$) when measured between -70 and -100 mV. However, DHPG currents were associated with a negative slope conductance in SNR neurons (0.8 $\pm$ 0.3 nS between -70 and -100 mV; $n = 10$) and SNC neurons (1.2 $\pm$ 0.5 nS between -60 and -90 mV; $n = 5$). The DHPG-evoked currents in STN neurons reversed polarity at -84.3 $\pm$ 2.0 mV. This reversal potential was more depolarized than expected for the K^+ equilibrium potential and was more hyperpolarized than expected for closing of a nonselective cationic conductance (Congar et al., 1997). These data suggest that DHPG-evoked currents may be mediated by more than one ionic conductance in STN neurons.

DHPG Evokes Sulfonylurea-Sensitive Currents in STN Neurons. We next investigated the ability of sulfonylurea agents to block outward currents evoked by DHPG. As shown in Fig. 2A, outward current evoked by DHPG (20 μM) was replaced by a small inward current in the presence of tolbutamide (100 μM). On average, DHPG evoked 95 $\pm$ 23 pA of outward current at -70 mV under control conditions ($n = 11$). In the presence of tolbutamide, however, DHPG evoked an inward current of 22 $\pm$ 4 pA in those same neurons ($P < 0.01$, paired t test). As shown in Fig. 2B, we used a series of hyperpolarizing voltage steps to measure the voltage-dependence of DHPG-evoked currents in the presence and absence of tolbutamide. We first investigated the effect of tolbutamide, applied alone, on membrane conductance. Fig. 2C shows that tolbutamide (100 μM) had a small but significant effect on membrane conductance in STN neurons ($n = 6$; $F_{1,7} = 18.80$, $P < 0.05$, two-way ANOVA with RM). The net current evoked by tolbutamide, shown in Fig. 2D, was obtained by subtracting currents evoked in tolbutamide from

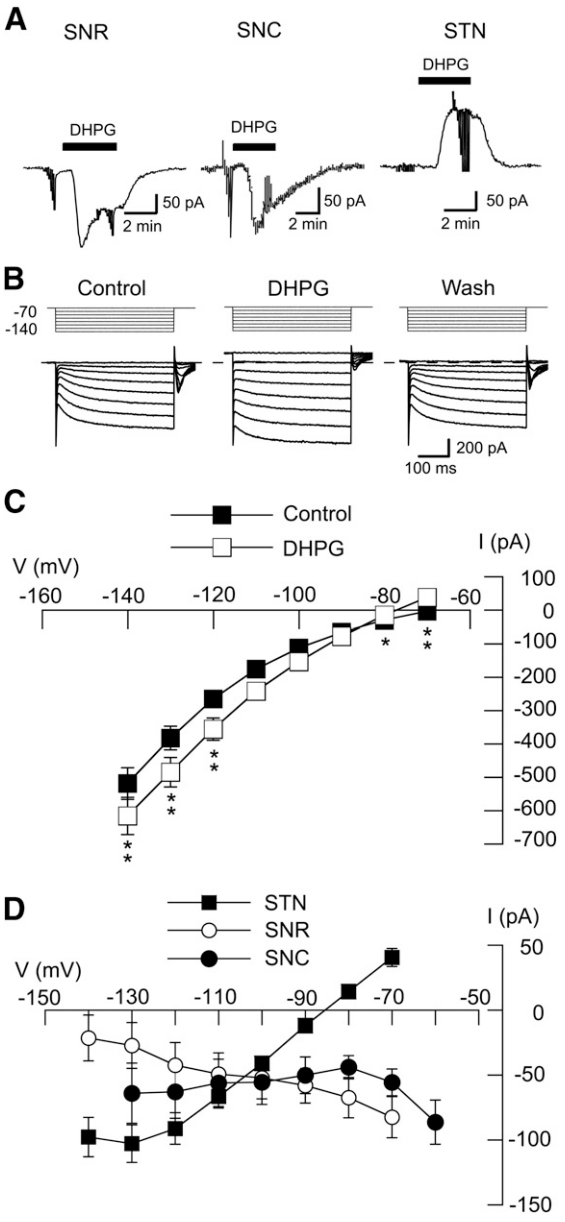

Fig. 1. DHPG increases conductance in STN neurons. (A) DHPG (20 μM) evokes inward currents in SNR (-70 mV) and SNC (-60 mV) neurons, but produces an outward current in an STN neuron (at -70 mV). Truncated deflections in these and subsequent current records are artifacts caused by voltage steps that were used to measure series resistance or membrane conductance. (B) Current traces recorded during a series of hyperpolarizing voltage steps (from -70 to -140 mV) show that DHPG (20 μM) increases membrane conductance in an STN neuron. Wash indicates recording after DHPG was washed from the slice. Dashed line indicates zero current. (C) Summarized I-V plots showing whole-cell conductance before (control) and during superfusion with 20 μM DHPG ($n = 25$). Significant differences: $^*P < 0.05$; $^{**}P < 0.01$; Holm-Sidak pairwise tests. (D) Summarized I-V plots showing net (subtracted) currents evoked by DHPG in STN ($n = 26$), SNR ($n = 10$), and SNC ($n = 5$) neurons. Note that DHPG increased conductance in STN neurons but not in SNR or SNC neurons.

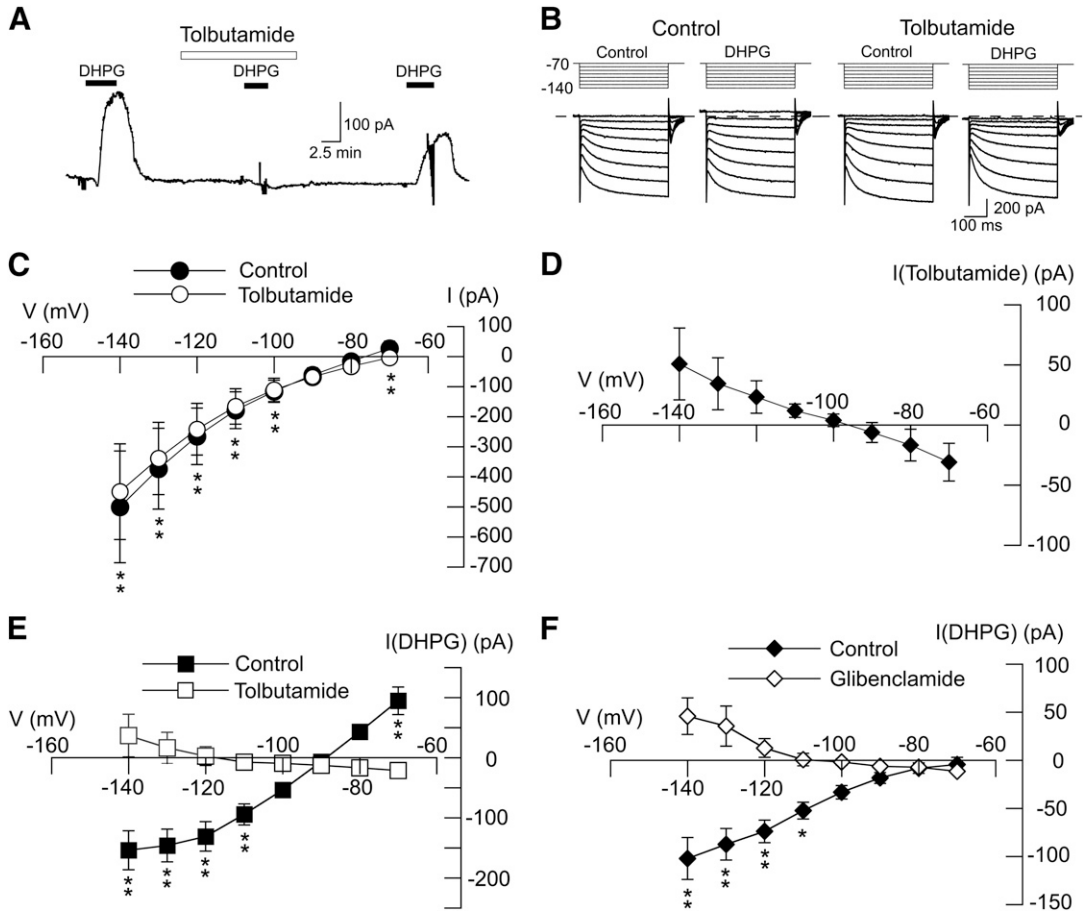

Fig. 2. DHPG-evokes sulfonylurea-sensitive currents in STN neurons. (A) Current trace shows that tolbutamide (100 μM) blocks DHPG-evoked outward current (at -70 mV). Note that DHPG caused a small inward current in the presence of tolbutamide. (B) Current traces recorded during a series of hyperpolarizing voltage steps (from -70 to -140 mV) show that the DHPG-evoked conductance increase is prevented by tolbutamide (100 μM). (C) I-V plots showing whole-cell conductance before (control) and during superfusion with 100 μM tolbutamide ($n = 6$). (D) I-V plot showing net (subtracted) currents evoked by tolbutamide; I-V plot was derived from data shown in (C). (E) I-V plots show that tolbutamide (100 μM) significantly altered the voltage-dependence of currents evoked by DHPG ($n = 11$; $P < 0.05$, two-way ANOVA with RM). Note that tolbutamide changed the slope conductance of DHPG-evoked currents from positive to negative. (F) I-V plots show that glibenclamide (1 μM) significantly altered voltage-dependence of currents evoked by DHPG ($n = 6$; $P < 0.01$, two-way ANOVA with RM). Significant differences at specific test potentials: $^*P < 0.05$; $^{**}P < 0.01$; Holm-Sidak tests.

those recorded before tolbutamide. Currents evoked by tolbutamide reversed at 95 $\pm$ 3 mV, which is consistent with an effect to block a resting K-ATP conductance. We then proceeded to study the ability of tolbutamide to block DHPG-induced currents. The resulting I-V plots in Fig. 2E show that tolbutamide significantly modified DHPG-induced currents ($F_{1,7} = 18.38$; $P < 0.05$, two-way ANOVA with RM). DHPG-induced current was associated with a positive slope conductance of 4.9 $\pm$ 1.0 nS when measured between -70 and -100 mV ($n = 11$). But in the presence of tolbutamide, DHPG currents were significantly altered, resulting in a negative slope conductance of 0.4 $\pm$ 0.1 nS ($n = 11$; $P < 0.01$, paired t test). In the presence of tolbutamide, DHPG-induced currents reversed at -107 ± 6 mV ($n = 6$), which is near the K^+ equilibrium potential; however, DHPG-induced inward currents did not reverse direction in five other neurons. As shown in the I-V plots in Fig. 2F, a second sulfonylurea agent, glibenclamide (1 μM), also significantly modified the DHPG I-V relationship ($n = 6$; $F_{1,7} = 13.03$; $P < 0.01$). Under control conditions, DHPG current was associated with a positive slope conductance of 1.0 $\pm$ 0.2 nS ($n = 6$). But in the presence of glibenclamide (1 μM), DHPG-induced current was significantly altered, resulting in a negative slope conductance of 0.3 $\pm$ 0.1 nS ($P < 0.01$, paired t test). DHPG-induced currents reversed at -109 ± 9 mV in the presence of glibenclamide ($n = 6$), which is near the estimated reversal potential for K^+. These results show that the DHPG-induced increase in slope conductance is sulfonylurea sensitive. In the presence of a sulfonylurea agent, DHPG evoked a negative slope conductance with reversal near the K^+ equilibrium potential in most neurons. These data suggest that inward current evoked by DHPG is largely due to closure of a resting K^+ conductance.

Diazoxide Occludes DHPG-Induced Outward Current. We next examined the interaction of DHPG-evoked current with currents evoked by the K-ATP channel opener diazoxide. As illustrated with the current trace in Fig. 3A, superfusing the slice with 20 μM DHPG for 5 minutes evoked an average outward current of 99 $\pm$ 17 pA at -70 mV ($n = 6$). However, DHPG (20 μM) evoked an inward current of 40 $\pm$ 7 pA in the same neurons when applied in the presence of 300 μM diazoxide ($P < 0.01$, paired t test). Diazoxide also altered the DHPG I-V relationship, as shown in Fig. 2B ($n = 6$; $P < 0.05$; $F_{1,7} = 46.79$). Under control conditions, DHPG current

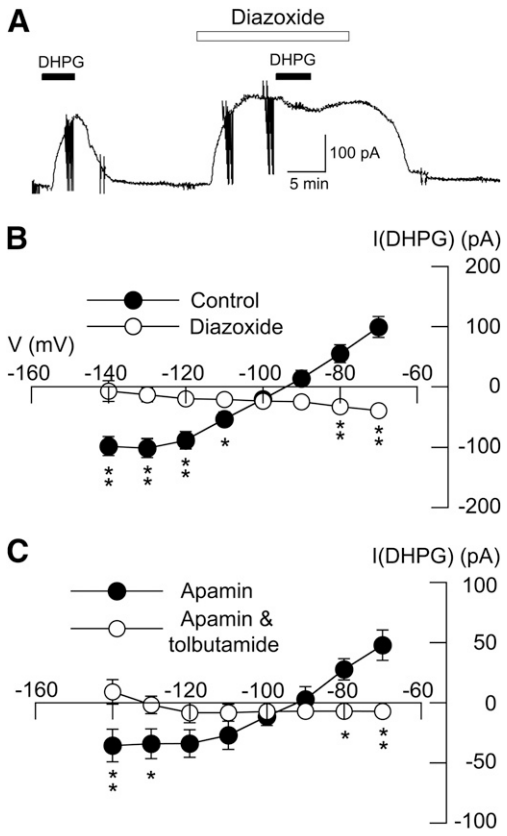

Fig. 3. Diazoxide (300 μM) occludes DHPG-induced outward current. (A) Continuous current trace (at −70 mV) shows that outward current evoked by DHPG (20 μM) is occluded by outward current evoked by the K-ATP channel opener diazoxide. (B) I-V plots for the action of 20 μM DHPG before (control) and in the presence of diazoxide. Diazoxide significantly altered the DHPG I-V plot (n = 6). (C) I-V plots for a control experiment showing lack of effect of apamin (1 μM) on tolbutamide-sensitive current evoked by DHPG. Tolbutamide antagonized DHPG-evoked currents in the continued presence of apamin. Significant differences at specific test potentials: $^*P < 0.05$; $^{**}P < 0.01$; Holm-Sidak tests.

was associated with a positive slope conductance of 4.0 ± 0.5 nS (n = 6). But when applied with diazoxide, DHPG current was significantly altered, resulting in a negative slope conductance of 0.6 ± 0.2 nS ($P < 0.001$, paired t test). These results suggest that K-ATP current evoked by DHPG can be occluded by current evoked by diazoxide. Taken together, these results indicate that outward current evoked by DHPG is mediated by K-ATP channels.

As a control experiment, we tested the ability of apamin, a blocker of small conductance Ca^{2+}-activated K^+ (gKCa) channels, to alter DHPG-induced current. In the presence of apamin (1 μM), DHPG (20 μM) evoked 48 ± 13 pA of outward current (at −70 mV); however, DHPG evoked an inward current of 7 ± 4 pA in the presence of tolbutamide (100 μM) plus apamin in those same neurons (n = 4; $P < 0.01$, paired t test). As summarized in the I-V plots in Fig. 3C, DHPG-evoked currents in apamin were associated with a positive slope conductance of 2.1 ± 0.3 nS (n = 4). Tolbutamide reduced the DHPG-induced conductance to 0 ± 0.2 nS in the continued presence of apamin ($P < 0.05$, paired t test). These data indicate that the conductance increase produced by DHPG is mediated by K-ATP channels and not by small conductance Ca^{2+}-activated K+ channels.

DHPG Receptor Pharmacology. A recent advance in mGluR pharmacology has been the discovery of negative allosteric modulators that act as noncompetitive glutamate antagonists (Marino and Conn, 2006). We used selective negative allosteric modulators to characterize the receptor pharmacology of inward and outward currents evoked by DHPG in STN neurons. In the presence of tolbutamide (100 μM), inward currents evoked by DHPG (20 μM) could be partially blocked by the mGluR5 negative modulator MPEP (10 μM), as shown in Fig. 4A. Moreover, the addition of the mGluR1 negative modulator CPCCOEt (100 μM) caused a further reduction in DHPG inward current. A summary of these experiments is shown in Fig. 4B. On average, the mGluR5 negative allosteric modulators MPEP (10 μM) and MTEP (10 μM) reduced DHPG-induced inward currents by 36 ± 4% (n = 10) and 32 ± 8% (n = 4), respectively. In contrast, the selective mGluR1 negative allosteric modulators CPCCOEt (100 μM) and JNJ16259685 (10 μM) reduced DHPG-induced inward currents by 55 ± 4% (n = 9) and 53 ± 2% (n = 6), respectively. Concurrent application of mGluR1 and mGluR5 negative modulators caused a larger reduction in DHPG-induced inward currents. Thus, concurrent application of MPEP (10 μM) and CPCCOEt (100 μM), or MTEP (10 μM) and JNJ16259685 (10 μM), reduced DHPG-induced inward currents by 65 ± 3% (n = 10) and 77 ± 3% (n = 9), respectively. These data suggest that both mGluR1 and mGluR5 receptors mediate inward currents evoked by DHPG.

We then proceeded to investigate effects of mGluR negative modulators on outward currents evoked by DHPG (Fig. 4C). When recording in the absence of tolbutamide, DHPG evoked an outward current at −70 mV that could be completely blocked by the combined application of MTEP (10 μM) and JNJ16259685 (10 μM). On average, DHPG evoked a 26 ± 12 pA of outward current under control conditions (n = 8), which was significantly different from the 14 ± 2 pA of inward current that was evoked in the presence of MTEP and JNJ16259685 in the same neurons ($P < 0.05$, paired t test). Concurrent application of MTEP and JNJ16259685 also significantly modified the voltage dependence of DHPG current, as seen in Fig. 4D ($F_{1,7} = 30.37$; $P < 0.05$). Under control conditions, DHPG current was associated with a positive slope conductance of 1.2 ± 0.3 nS (n = 8). But in the presence of MTEP and JNJ16259685, the DHPG I-V plot yielded a negative slope conductance of 0.5 ± 0.1 nS ($P < 0.01$, paired t test). These results suggest that mGluR1 and mGluR5 receptors mediate DHPG-induced outward currents as well as inward currents in STN neurons.

DHPG-Evoked Conductance Increase is Mediated by Intracellular Ca^{2+} Release. It is well-established that activation of group I mGluRs increases levels of intracellular Ca^{2+} by promoting release of Ca^{2+} from intracellular stores (Abe et al., 1992; Fagni et al., 2000). Moreover, we previously showed that Ca $^{2+}$ influx through NMDA-gated channels activates K-ATP channels in STN neurons (Shen and Johnson, 2010). Therefore, we explored whether Ca^{2+} mobilization might be necessary for activation of K-ATP channels by DHPG. We first examined caffeine, which is widely used as an activator of Ca^{2+} release from intracellular stores (Henzi and MacDermott, 1992). As seen in the current trace in Fig. 5A, caffeine (1 mM in superfusate) evoked a tolbutamide-sensitive outward current at −70 mV. On average, caffeine evoked 48 ± 25 pA of outward current at −70 mV, and this outward current

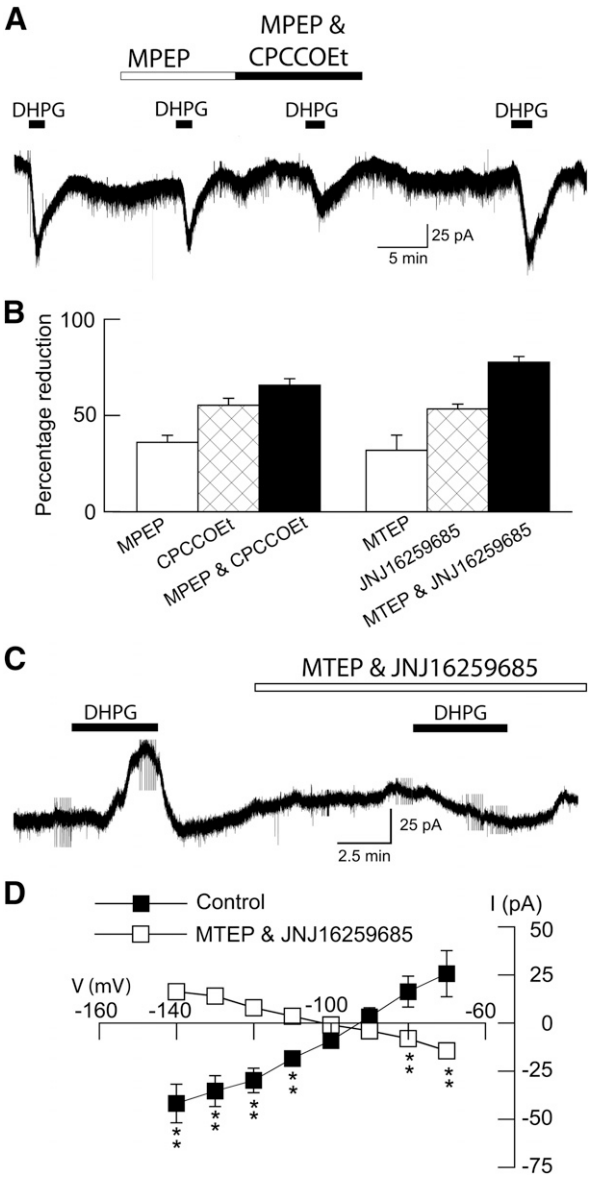

Fig. 4. DHPG activates both mGluR1 and mGluR5 receptors. (A) Continuous current trace shows that DHPG-evoked inward currents are partially blocked by MPEP (20 μM) and CPCCOEt (100 μM). Recordings were done in the presence of tolbutamide (100 μM) to block K-ATP currents. (B) Bar graph summarizing the blockade of DHPG-evoked inward currents by mGluR1 (CPCCOEt, 100 μM; JNJ16259685, 10 μM) and mGluR5 (MPEP, 20 μM; MTEP, 10 μM) negative allosteric modulators. All recordings were done in tolbutamide and AP5. Each bar represents the mean of 4–10 cells. (C) Continuous current trace, recorded in the absence of tolbutamide and AP5, shows that outward current evoked by DHPG (20 μM) is blocked by concurrent application of JNJ16259685 (10 μM) and MTEP (10 μM). (D) I-V plots show that JNJ16259685 plus MTEP significantly altered the voltage dependence of currents evoked by DHPG ($P < 0.05$, two-way ANOVA with RM). Note that superfusion with mGluR1 and mGluR5 modulators changed the slope conductance of DHPG-evoked currents from positive to negative ($n = 8$). $^{**}P < 0.01$; Holm-Sidak tests.

was reduced to 1 ± 2 pA by 100 μM tolbutamide ($n = 5$, $P < 0.05$, paired t test). The voltage-dependence of caffeine-evoked currents was also significantly altered by tolbutamide ($F_{1,7} = 13.64$; $P < 0.05$) as shown in Fig. 5B. On average, current evoked by caffeine was associated with a positive slope conductance of 4.0 ± 0.8 nS. However, caffeine-dependent slope conductance was reduced to 0.4 ± 0.1 nS in the presence of tolbutamide ($n = 5$; $P < 0.05$, paired t test). These data suggest that intracellular Ca^{2+} mobilization can evoke K-ATP current in STN neurons.

We proceeded to test whether agents that deplete intracellular Ca^{2+} can interfere with outward current generated by DHPG. Fig. 5C shows that cyclopiazonic acid, which blocks ATPase-mediated Ca^{2+} uptake (Suzuki et al., 1992), completely blocked outward current evoked by 20 μM DHPG at −70 mV. On average, DHPG evoked an outward current of 26 ± 10 pA at −70 mV under control conditions ($n = 7$), whereas DHPG evoked an inward current of 22 ± 4 pA in the presence of 10 μM cyclopiazonic acid ($P < 0.01$, paired t test). Cyclopiazonic acid also modified the DHPG I-V relationship ($F_{1,7} = 24.78$; $P < 0.05$), as seen in Fig. 5D. Under control conditions, DHPG current was associated with a positive slope conductance of 1.5 ± 0.3 nS ($n = 7$). But in the presence of cyclopiazonic acid, DHPG current was significantly altered with a negative slope conductance of 0.4 ± 0.2 nS ($P < 0.001$, paired t test).

We obtained similar results with thapsigargin, which causes depletion of intracellular Ca^{2+} stores by inhibiting ATPase-mediated Ca^{2+} uptake into endoplasmic reticulum (Thastrup et al., 1990). In these experiments, test responses to DHPG (20 μM) were recorded at 20- to 30-minute intervals after starting whole-cell recordings with pipettes that contained thapsigargin (3 μM). As shown in Fig. 5E, intracellular dialysis of thapsigargin gradually blocked outward current evoked by DHPG. On average, the initial application of DHPG (20 μM) evoked an outward current of 70 ± 36 pA at −70 mV. However, DHPG evoked 26 ± 6 pA of inward current after 20–30 minutes of dialysis with thapsigargin ($n = 6$; $P < 0.05$, paired t test). Intracellular dialysis of thapsigargin also significantly modified the DHPG I-V relationship ($F_{1,7} = 20.34$; $P < 0.05$), as shown in Fig. 5F. On average, the initial application of DHPG evoked currents with a positive slope conductance of 2.7 ± 1.3 nS. However, after more than 20 minutes dialysis with thapsigargin, DHPG-evoked current was significantly altered, with a negative slope conductance of 0.5 ± 0.2 nS ($n = 6$; $P < 0.05$, paired t test). As a control experiment, we examined effects of repetitive applications of DHPG on currents recorded with pipettes that contained normal internal solution. As shown in Fig. 5G, repetitive applications of DHPG consistently evoked comparable outward currents at −70 mV. Fig. 5H shows that the I-V relationship for the response to the second DHPG application was not significantly different from the response to the first DHPG application ($n = 5$; $F_{1,7} = 0.64$; $P = 0.4$). Thus, inhibition of DHPG-induced currents by thapsigargin cannot be attributed to a gradual run-down due to repeated applications of DHPG. Inhibition by thapsigargin is consistent with the hypothesis that intracellular Ca^{2+} is required for DHPG activation of K-ATP currents.

Involvement of Ryanodine- and $InsP_3$-sensitive Ca^{2+} Stores. Ryanodine and $InsP_3$ receptors regulate release of Ca^{2+} from intracellular stores, and block of these receptors interferes with Ca^{2+} release (Ehrlich et al., 1994). We tested the effects of ryanodine, which interferes with Ca^{2+} storage, as well as the $InsP_3$ receptor antagonist 2-APB, on outward current evoked by DHPG. Superfusing the brain slice with ryanodine (10 μM) caused a large reduction in outward

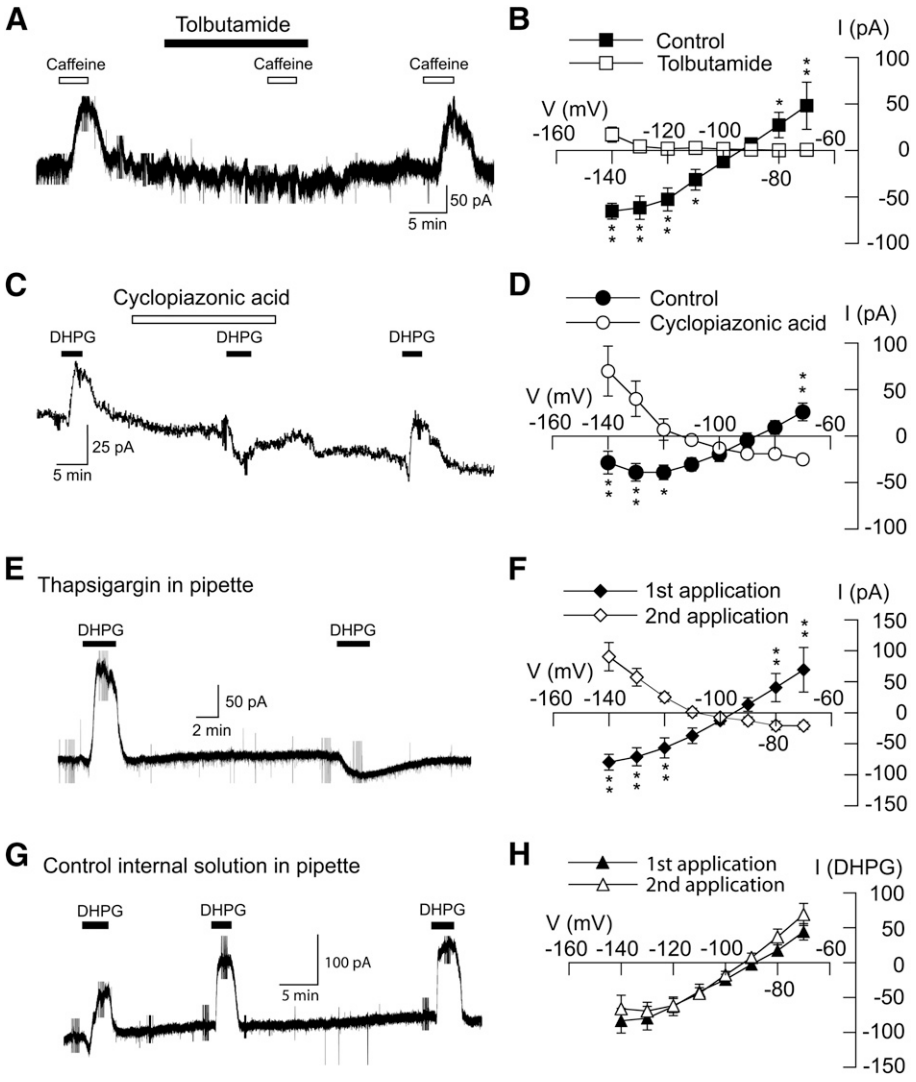

Fig. 5. Intracellular Ca^{2+} release is required for DHPG-evoked K-ATP conductance increase. (A) Current trace shows that caffeine (1 mM), which induces Ca^{2+} release from intracellular stores, mimicked DHPG by evoking a tolbutamide-sensitive outward current (at −70 mV) in an STN neuron. (B) I–V plots show that tolbutamide (100 μM) completely blocked the caffeine-induced conductance increase (n = 5; $P < 0.05$, two-way ANOVA with RM). (C) Current trace shows that cyclopiazonic acid (10 μM), which depletes intracellular Ca^{2+} stores, blocks DHPG-evoked outward current in an STN neuron at -70 mV. (D) I–V plots show that cyclopiazonic acid significantly altered the voltage dependence of DHPG current (n = 7; $P < 0.05$, two-way ANOVA with RM). (E) Current trace shows that intracellular dialysis with thapsigargin (3 μM), which depletes intracellular Ca^{2+} stores, blocks DHPG-evoked outward current at –70 mV. After 15 minutes of intracellular dialysis with thapsigargin, DHPG evoked an inward current. (F) I–V plots show that intracellular dialysis with thapsigargin significantly altered the voltage dependence of DHPG currents (n = 6; $P < 0.05$, two-way ANOVA with RM). (G) Current trace shows that repetitive application of DHPG consistently evokes an outward current at –70 mV in an STN neuron recorded with a pipette containing control internal solution. (H) Summarized I–V plots showing similar conductance increases evoked by repeat applications of DHPG in STN neurons with control solution in pipettes (n = 5). *$P < 0.05$; **$P < 0.01$; Holm-Sidak tests.

current evoked by DHPG (20 μM). On average, DHPG evoked 31 ± 13 pA of inward current in the presence of ryanodine, which was significantly different from the 14 ± 14 pA of outward current evoked by DHPG at −70 mV in control conditions (n = 5; $P < 0.01$, paired t test). The DHPG I-V relationship was also significantly modified by ryanodine ($F_{1,7}$ = 10.00; $P < 0.01$), as shown in Fig. 6A. Slope conductance for DHPG current in the presence of ryanodine (−1.0 ± 0.4 nS) was significantly different from that under control conditions (+0.6 ± 0.4 nS; n = 5; $P < 0.05$, paired t test).

The $InsP_3$ antagonist 2-APB also blocked DHPG-induced outward current, as shown in the current trace in Fig. 6B. 2-APB (200 μM) was added to the internal pipette solution, and slices were superfused for 5 minutes with DHPG (20 μM) every 20–30 minutes. On average, the initial application of DHPG evoked an outward current of 13 ± 7 pA at −70 mV. However, the second application of DHPG evoked 12 ± 2 pA of inward current during intracellular dialysis with 2-APB (n = 8; $P < 0.01$, paired t test). 2-APB also significantly modified the DHPG I-V relationship, as shown in Fig. 6C ($F_{1,7}$ = 17.74; $P < 0.05$). The initial application of DHPG evoked current with a positive slope conductance of 0.9 ± 0.2 nS. However, after 20–30 minutes dialysis with 2-APB, the second DHPG application evoked current with a negative slope conductance of 0.5 ± 0.2 nS (n = 8; $P < 0.001$, paired t test). These results further support the hypothesis that Ca^{2+} mobilization from intracellular stores is necessary for DHPG to evoke K-ATP current in STN neurons.

DHPG-dependent K-ATP Conductance Increase Requires NO. Previous studies have shown that NO can be generated by the increase in intracellular Ca^{2+} caused by group I mGluR stimulation (Caruso et al., 2006; Sergeeva et al., 2007). Because NO is a known facilitator of K-ATP channel activation (Shinbo and Iijima, 1997; Kawano et al., 2009), we next explored the effect of the nitric oxide synthase (NOS) inhibitor L-NAME on DHPG-evoked outward current. As shown in Fig. 7A, superfusing with L-NAME (200 μM) for 15 minutes completely blocked the outward current evoked by DHPG (20 μM) at −70 mV. On average, DHPG evoked an inward current of 29 ± 18 pA at −70 mV in the presence of L-NAME, which was significantly different from the 69 ± 14 pA of outward current that was evoked by DHPG under control conditions in the same neurons (n = 8; $P < 0.01$, paired t test). L-NAME also significantly modified the DHPG I-V relationship, as shown in Fig. 7B ($F_{1,7}$ = 10.80; $P < 0.05$). Under control conditions, DHPG current was

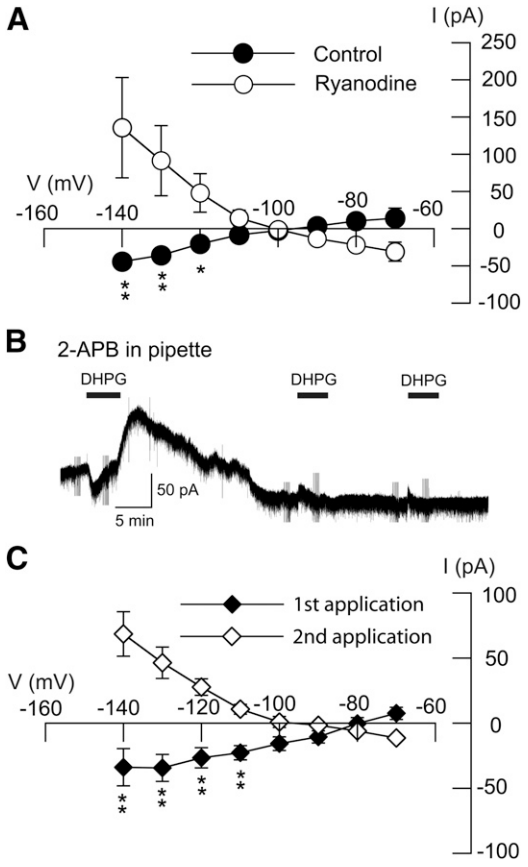

Fig. 6. Ryanodine- and $InsP_3$-gated Ca^{2+} release are required for DHPG-induced conductance increase. (A) I–V plots showing that bath application of ryanodine (10 μM) significantly altered the DHPG I-V plot ($n = 5$; $P < 0.01$; two-way ANOVA with RM). (B) Current trace shows that intracellular dialysis of 2-APB (200 μM), an $InsP_3$ receptor antagonist, blocked DHPG-evoked outward current at –70 mV. (C) I–V plots show that intracellular dialysis of 2-APB significantly altered the DHPG I-V plot over time ($n = 8$; $P < 0.05$, two-way ANOVA with RM). *$P < 0.05$; **$P < 0.01$; Holm-Sidak tests.

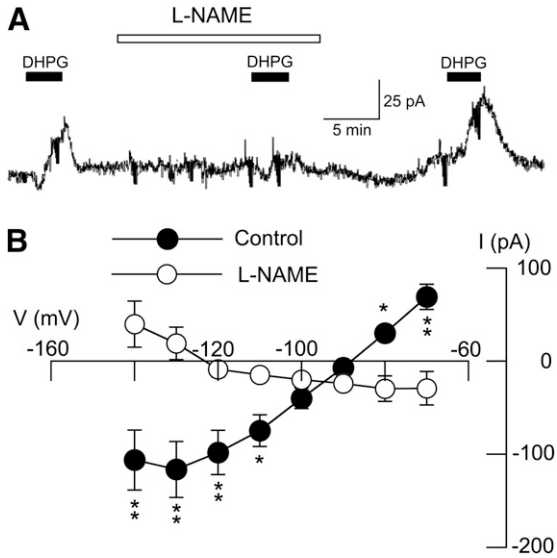

Fig. 7. DHPG-evoked K-ATP conductance increase requires NO. (A) Current traces show that DHPG-evoked outward current (at −70 mV) is blocked by the NOS inhibitor L-NAME (200 μM). Note that DHPG caused an inward current in the presence of tolbutamide. (B) I-V plots show that L-NAME (200 μM) significantly altered the voltage-dependence of currents evoked by DHPG ($P < 0.05$, two-way ANOVA with RM). Note that L-NAME changed the slope conductance of DHPG-evoked currents from positive to negative ($n = 8$). Significant differences at specific test potentials: *$P < 0.05$; **$P < 0.01$; Holm-Sidak tests.

associated with a positive slope conductance of 3.7 ± 0.8 nS. However, in the presence of L-NAME, the DHPG I-V plot had a significantly different negative slope conductance of 0.3 ± 0.6 nS ($n = 8$; $P < 0.01$, paired t test). These results suggest that NO is required for generation of K-ATP current by DHPG.

cGMP-dependent Protein Kinase Mediates DHPG-dependent K-ATP Conductance Increase. Because NO has been shown to activate K-ATP channels via the cGMP-dependent protein kinase (PKG) (Han et al., 2001; Brito et al., 2006), we next investigated the role of PKG in the activation of K-ATP current by DHPG. We made whole-cell recordings with pipettes that contained the guanylyl cyclase inhibitors ODQ (20 μM) or LY83583 (20 μM) or the PKG inhibitor Rp-8-Br-PET-cGMPs (50 μM). Test responses to DHPG (20 μM) were recorded at 20- to 30-minute intervals after starting whole-cell recordings. As seen in Fig. 8A, intracellular dialysis of ODQ greatly reduced DHPG-evoked outward current over time. On average, the initial application of DHPG (20 μM) evoked an outward current of 60 ± 17 pA at −70 mV. In contrast, DHPG evoked inward current (28 ± 7 pA, $n = 8$) after 20–30 minutes of intracellular dialysis with ODQ ($P < 0.01$, paired t test). Intracellular ODQ also significantly modified the I-V relationship of DHPG currents, as seen in Fig. 8B ($F_{1,7} = 10.77$; $P < 0.05$). On average, the initial application of DHPG evoked current with a positive slope conductance of 3.6 ± 1.1 nS, which was significantly different from the negative slope conductance of 1.0 ± 0.2 nS after 20–30 minute of ODQ dialysis ($n = 8$; $P < 0.01$, paired t test). The guanylyl cyclase inhibitor LY83583 also caused time-dependent inhibition of DHPG current, as seen in Fig. 8C. The I-V plot in Fig. 8D shows that intracellular dialysis of LY83583 (20 μM) significantly changed the voltage-dependent responses to repeat applications of DHPG ($F_{1,7} = 5.08$; $P < 0.01$). On average, the initial application of DHPG evoked current with a positive slope conductance of 0.5 ± 0.2 nS. However, after more than 20 minutes dialysis of LY83583, DHPG current was significantly different, with a negative slope conductance of 0.5 ± 0.2 nS ($n = 6$; $P < 0.05$, paired t test). Finally, we explored effects of the PKG inhibitor Rp-8-Br-PET-cGMPs on currents evoked by DHPG. As shown in the current trace in Fig. 8E, intracellular dialysis of Rp-8-Br-PET-cGMPs (50 μM) greatly reduced the outward current evoked by DHPG. On the first application, DHPG evoked an outward current of 51 ± 18 pA at −70 mV. In contrast, DHPG-evoked an inward current (5 ± 5 pA, $n = 7$) when recorded at least 20 minutes after starting whole-cell recording ($P < 0.05$, paired t test). Intracellular dialysis of Rp-8-Br-PET-cGMPs also significantly modified the DHPG I-V relationship ($F_{1,7} = 19.53$; $P < 0.01$), as shown in Fig. 8F. On average, the first application of DHPG evoked current with a positive slope conductance of 3.2 ± 1.0 nS. However, the slope conductance was reduced to 0.1 ± 0.3 nS 20–30 minutes after starting whole-cell recording with Rp-8-Br-PET-cGMPs in pipettes ($n = 7$; $P < 0.01$, paired t test). These results suggest that PKG is required for activation of K-ATP channels by DHPG.

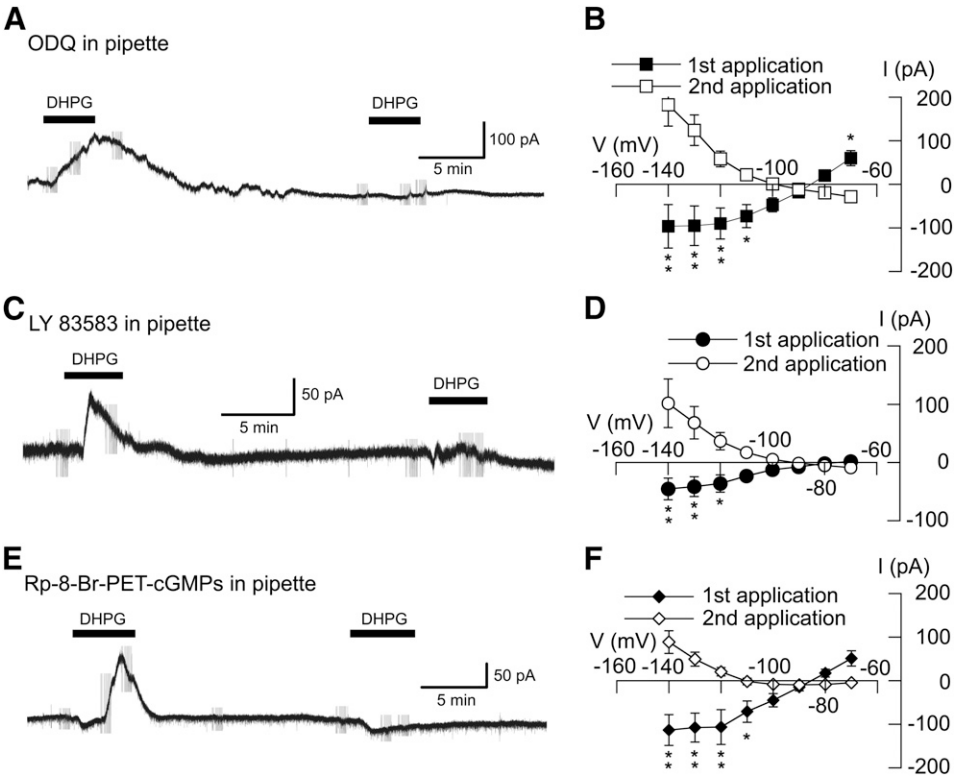

Fig. 8. DHPG-evoked K-ATP conductance increase requires activation of PKG. (A) current trace shows that intracellular dialysis of the guanylyl cyclase inhibitor ODQ (20 μM) blocks DHPG-evoked outward current at –70 mV. After 15 minutes of intracellular dialysis with ODQ, DHPG evoked a small inward current. (B) I–V plots show that intracellular dialysis of ODQ significantly altered the voltage dependence of currents evoked by DHPG (n = 8). (C) Current trace shows that intracellular dialysis of the guanylyl cyclase inhibitor LY83583 (20 μM) blocks DHPG-evoked outward current at –70 mV. After 15 minutes of intracellular dialysis with LY83583, DHPG evoked a small inward current. (D) I–V plots show that intracellular dialysis of LY83583 significantly altered the voltage dependence of DHPG currents (n = 6). (E) Current trace shows that intracellular dialysis of the PKG inhibitor Rp-8-Br-PET-cGMPs (50 μM) blocked DHPG-evoked outward current at −70 mV. After 15 minutes of intracellular dialysis with Rp-8-Br-PET-cGMPs, DHPG evoked a small inward current. (F) I–V plots show that intracellular dialysis of Rp-8-Br-PET-cGMPs significantly altered the I-V plot of DHPG currents (n = 7). *$P < 0.05$; **$P < 0.01$; Holm-Sidak tests.

Functional Consequences of K-ATP Channel Activation by DHPG. We used the loose-patch recording technique to examine the effects of DHPG on spontaneous action potential discharge rate in the presence and absence of tolbutamide. As shown in Fig. 9A, superfusing the slice with DHPG (20 μM) for 5 minutes caused a small increase in firing rate, from a control value of 10.4 ± 2.0 Hz to 12.9 ± 3.4 Hz (n = 7). But in tolbutamide, DHPG increased firing rate to 22.3 ± 3.0 Hz, which was significantly greater than the control DHPG effect ($P < 0.001$, paired t test). Figure 9B shows the averaged effects of DHPG with and without tolbutamide on firing rate over time; this graph shows that tolbutamide produced a significant augmentation in DHPG-evoked firing rate in STN neurons (n = 7; $F_{1,103} = 4.531$; $P < 0.001$).

In addition to firing rate, firing pattern of STN neurons is another parameter that strongly impacts locomotor activity (Bevan et al., 2002). Furthermore, the burst firing pattern is well known to be generated by depolarizing plateau potentials in STN neurons (Beurrier et al., 1999; Bevan and Wilson, 1999; Otsuka et al., 2001; Baufreton et al., 2003; Kass and Mintz, 2006). We used current-clamp recordings in the whole-cell configuration to examine the effect of DHPG on the duration of plateau potentials that were evoked by 100-ms pulses of depolarizing current. Plateau potential duration was measured as the time from depolarization onset to return to baseline. Small amounts of current were injected as needed to maintain resting potential at −70 mV during DHPG and tolbutamide applications. As seen in the current traces in Fig. 10A, DHPG (20 μM) had little effect on plateau potential duration when applied alone. However, DHPG greatly prolonged the plateau potential duration when recorded in tolbutamide (100 μM). Averaged responses are shown in Fig. 10B. DHPG (20 μM) caused a small but significant reduction in plateau potential duration from a control duration of 239 ± 18 ms to 169 ± 11 ms (n = 8; $P < 0.01$, paired t test). DHPG also reduced the number of evoked spikes to 2.8 ± 1.1 from a control value of 6.9 ± 0.6 ($P < 0.01$, paired t test). But in the presence of tolbutamide (100 μM), DHPG caused a marked prolongation of plateau potential duration, from a control duration of 325 ± 60 ms to 582 ± 179 ms (n = 8; $P < 0.05$, paired t test). Tolbutamide applied alone increased plateau duration but this was not statistically significant (P = 0.18). In tolbutamide, DHPG also increased the number of evoked spikes to 13.9 ± 6.7 from a control value of 8.1 ± 2.0, but this increase was not statistically significant (P = 0.26). Taken together, these results suggest that K-ATP currents evoked by group I mGluRs can influence STN neuronal activity, and the excitatory effect of mGluR activation can be uncovered when K-ATP channels are blocked.

Discussion

Our results show that the group I mGluR agonist DHPG evokes both inward and outward currents in rat STN neurons. These currents are largely blocked by mGluR1 and mGluR5 negative allosteric modulators, which suggest that both currents are generated by the same subtypes of receptor. Outward current evoked by DHPG was identified as K-ATP current because it was blocked by the K-ATP channel blockers tolbutamide and glibenclamide. Inhibitors of $InsP_3$- and ryanodine-sensitive pathways prevented the activation of K-ATP current by DHPG, which suggests that this current requires mobilization of Ca^{2+} from intracellular stores. K-ATP activation was also blocked by inhibitors of NOS and PKG. These results are similar to our previous studies showing that NMDA evoked K-ATP current in STN neurons by Ca^{2+} influx

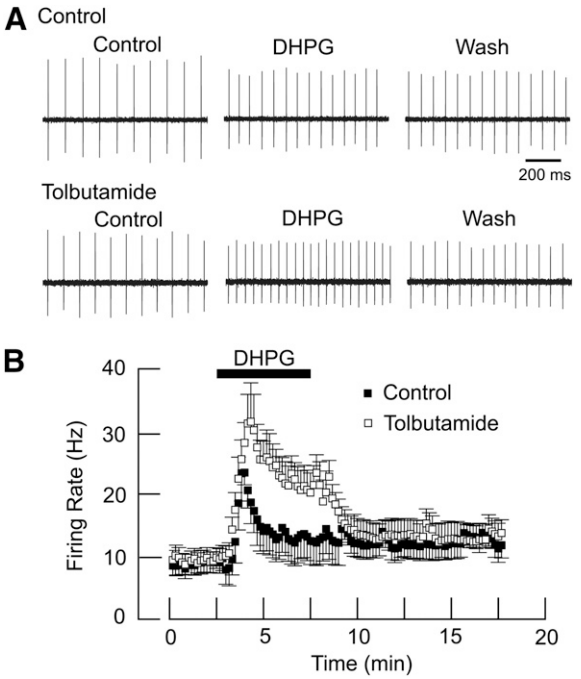

Fig. 9. Loose-patch recordings show that tolbutamide augments DHPG-dependent acceleration of firing rate. (A) Representative voltage traces showing firing rate before and after DHPG (20 μM) in the absence and presence of tolbutamide (100 μM). DHPG was superfused for 5 minutes, and tolbutamide was superfused 10 minutes prior to repeat application of DHPG. Note that the excitatory effect of DHPG is more pronounced in the presence of tolbutamide. (B) Averaged responses showing that tolbutamide significantly potentiated the DHPG-induced increase in firing rate ($n = 7$; $P < 0.001$).

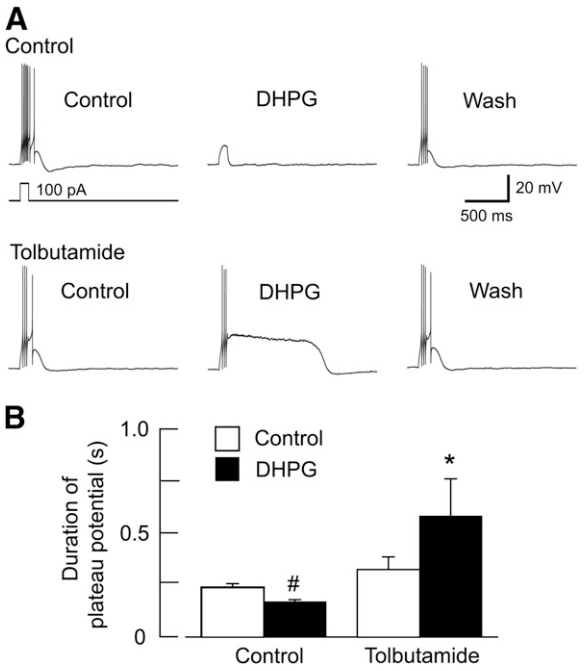

Fig. 10. DHPG prolongs plateau potentials in the presence of tolbutamide. (A) Whole-cell current-clamp recordings of an STN neuron showing that block of K-ATP channels by tolbutamide (100 μM) potentiates the ability of DHPG to prolong depolarizing plateau potentials. All voltage traces are from the same STN neuron. Plateau potentials were evoked by a 100-pA depolarizing current pulse lasting 100 milliseconds; a small hyperpolarizing holding current was applied to establish an initial membrane potential of -70 mV. Wash indicates recording after DHPG is washed from the slice. (B) Summary graph showing that DHPG significantly prolonged plateau potentials in the presence of tolbutamide ($n = 8$; $^*P < 0.05$, paired t test). Note that DHPG caused a small reduction in plateau potential duration in the absence of tolbutamide ($\#P < 0.01$, paired t test).

with subsequent activation of NOS and PKG (Shen and Johnson, 2010). Thus, it would appear that Ca^{2+}-dependent activation of K-ATP channels can be triggered by more than one glutamate receptor subtype. To our knowledge, our study is the first to report that K-ATP current can be evoked by mGluR stimulation by a process involving release of Ca^{2+} from intracellular stores in a central neuron.

Group I mGluRs have been reported previously to evoke Ca^{2+}-dependent outward currents or membrane hyperpolarization in a variety of cells, but these have been reports in which mGluRs activate Ca^{2+}-dependent K^+ (gKCa) currents. For example, Fiorillo and Williams (1998) reported that mGluR1 stimulation evoked a late inhibitory postsynaptic current in midbrain dopamine neurons. Although this late inhibitory postsynaptic current was dependent upon Ca^{2+} release from $InsP_3$- and ryanodine-sensitive calcium stores, the outward current was mediated by apamin-sensitive Ca^{2+}-activated K+ channels rather than K-ATP channels (Fiorillo and Williams, 1998). A gKCa-mediated inhibitory postsynaptic current has also been described in basolateral amygdala neurons that is dependent upon a thapsigargin-sensitive release of intracellular Ca^{2+} by group I mGluR stimulation (Rainnie et al., 1994). Sharifullina et al. (2005) reported that DHPG-induced membrane oscillations and burst firing were blocked by a sulfonylurea agent in hypoglossal neurons, but they ascribed the K-ATP current to reduced levels of intracellular ATP. There are other studies in which group I mGluR stimulation reportedly inhibited K-ATP channel activity. For example, Mironov and Richter (2000) reported that K-ATP single channel activity in brain stem respiratory control neurons was inhibited by group I mGluR agonists that acted via a G protein-coupled mechanism. Moreover, mGluR5 stimulation has been reported to inhibit insulin secretion from pancreatic beta cells by a mechanism involving reduced K-ATP channel function (Brice et al., 2002). In reviewing the literature cited above, it should be clear that group I mGluR activation will have different actions depending upon the presence or absence of coupling to specific ion channels and differential regulation by second messenger systems. To our knowledge, ours is the first study to show that K-ATP current can be evoked by group I mGluR stimulation by a mechanism involving release of Ca^{2+} from intracellular stores in a central neuron.

Our studies showed that DHPG evoked K-ATP currents in STN but not in SNC or SNR neurons. This is curious, because both SNC and SNR neurons are known to express group I mGluRs (Messenger et al., 2002) and K-ATP channels (Karschin et al., 1997; Dunn-Meynell et al., 1998). It is not clear why mGluR stimulation failed to evoke K-ATP currents in SNC and SNR neurons, but this could be due to differences in coupling of receptors to second messenger systems or to differences in subcellular localizations of mGluRs and K-ATP channels. Although STN neurons may not be unique in this regard, our results suggest that mGluRs are functionally coupled to K-ATP channels in STN neurons in ways that are not shared by SNC and SNR neurons.

Results of our studies confirm those of Awad et al. (2000) who reported that DHPG evokes inward current in STN neurons in slices of rat brain. In the presence of a sulfonylurea agent, we found that DHPG increased a negative slope conductance that reversed near the expected K^+ equilibrium potential in most neurons; this observation agrees with the conclusion by Awad et al. (2000) that DHPG-induced inward current is largely caused by a reduction in a resting K^+ conductance. However, our results also differ from theirs in several aspects. First, Awad et al. reported that DHPG evoked current by activation of the mGluR5 but not the mGluR1 subtype; this is despite the fact that both mGluR5 and mGluR1 have been shown to be expressed by STN neurons (Wang et al., 2000; Kuwajima et al., 2004, 2007). Moreover, activation of either receptor subtype has been shown to increase intracellular levels of Ca^{2+} in STN neurons (Marino et al., 2002). By showing that both mGluR1 and mGluR5 evoke inward current, our results suggest that both mGluR subtypes have physiologic function in the STN. Second, Awad et al. reported that DHPG evoked inward current but not outward current in STN neurons. Because K-ATP activation by DHPG requires release of intracellular stores of Ca^{2+}, we purposely used pipette solutions that did not strongly buffer Ca^{2+}. However, the pipette solution used by Awad et al. contained a low concentration of EGTA (0.2 mM), which was the same that we used in the present study. Although differences in Ca^{2+} buffering did not appear to be significant, there was a significant difference in age of animals used in experiments. Whereas we used slices prepared from adult rats, Awad et al. (2000) used rats that were only 10–14 days old. Several studies have shown that specific glibenclamide binding sites in basal ganglia are much reduced in neonatal brain compared with adult rat brain (Mourre et al., 1990; Xia and Haddad, 1991). Furthermore, Liss et al. (1999, 2005) showed that substantia nigra dopamine neurons from young (P14) mice express the SUR2B subunit of the K-ATP channel, whereas adult mice only express the SUR1 subtype. Thus, it is possible that neonatal central neurons might express K-ATP channel subunits that differ from those expressed in adult brain. Moreover, K-ATP channels containing the SUR2B subunit are less sensitive to sulfonylurea block and have other significant pharmacological differences compared with K-ATP channels that contain SUR1 subunits (Aguilar-Bryan and Bryan, 1999). It is possible that DHPG does not evoke K-ATP currents in neonatal STN neurons due to lack of sufficient K-ATP channel expression or to expression of alternate K-ATP subunits.

Conclusions

Our results show that group I mGluR stimulation has dual effects by evoking both excitatory and inhibitory currents in STN neurons. Furthermore, our previous study demonstrated that Ca^{2+} influx through NMDA-gated channels can also activate K-ATP channels (Shen and Johnson, 2010). Although the relative influences of mGluR and NMDA receptor activation on STN neuronal activity are not known, the fact that both of these receptors trigger K-ATP current suggests that K-ATP channels can attenuate the excitatory influence of these receptors. In Parkinson's disease, when there is increased burst firing of STN neurons, it is possible that K-ATP currents may therefore resist the worsening of parkinsonian symptoms that are associated with burst firing. Thus, the present and our previous works show that K-ATP currents shorten the duration of depolarizing plateau potentials and curtail NMDA-induced burst firing in STN neurons (Shen and Johnson, 2010). Moreover, chronic dopamine depletion caused by intracerebral 6-hydroxydopamine treatment has been shown to increase the expression of K-ATP channel subunits in rat basal ganglia (Wang et al., 2005). In agreement, a recent study from our laboratory showed that chronic dopamine depletion potentiates the ability of NMDA receptor stimulation to evoke K-ATP currents and to inhibit spontaneous firing rate of rat STN neurons (Shen and Johnson, 2012). These studies suggest that the influence of K-ATP channels in the STN may be increased in Parkinson's disease. Future studies will be needed to determine the degree to which K-ATP currents can modify the firing pattern of STN neurons during chronic dopamine depletion in the intact animal.

Authorship Contributions

Participated in research design: Shen, Johnson.
Conducted experiments: Shen.
Performed data analysis: Shen, Johnson.
Wrote or contributed to the writing of the manuscript: Shen, Johnson.

References

Abe T, Sugihara H, Nawa H, Shigemoto R, Mizuno N, and Nakanishi S (1992) Molecular characterization of a novel metabotropic glutamate receptor mGluR5 coupled to inositol phosphate/Ca^{2+} signal transduction. *J Biol Chem* **267**: 13361–13368.

Aguilar-Bryan L and Bryan J (1999) Molecular biology of adenosine triphosphate-sensitive potassium channels. *Endocr Rev* **20**:101–135.

Albin RL, Young AB, and Penney JB, Jr (1995) The functional anatomy of disorders of the basal ganglia. *Trends Neurosci* **18**:63–64.

Awad H, Hubert GW, Smith Y, Levey AI, and Conn PJ (2000) Activation of metabotropic glutamate receptor 5 has direct excitatory effects and potentiates NMDA receptor currents in neurons of the subthalamic nucleus. *J Neurosci* **20**:7871–7879.

Baufreton J, Garret M, Rivera A, de la Calle A, Gonon F, Dufy B, Bioulac B, and Taupignon A (2003) D5 (not D1) dopamine receptors potentiate burst-firing in neurons of the subthalamic nucleus by modulating an L-type calcium conductance. *J Neurosci* **23**:816–825.

Bergman H, Wichmann T, Karmon B, and DeLong MR (1994) The primate subthalamic nucleus. II. Neuronal activity in the MPTP model of parkinsonism. *J Neurophysiol* **72**:507–520.

Beurrier C, Congar P, Bioulac B, and Hammond C (1999) Subthalamic nucleus neurons switch from single-spike activity to burst-firing mode. *J Neurosci* **19**: 599–609.

Bevan MD, Magill PJ, Terman D, Bolam JP, and Wilson CJ (2002) Move to the rhythm: oscillations in the subthalamic nucleus-external globus pallidus network. *Trends Neurosci* **25**:525–531.

Bevan MD and Wilson CJ (1999) Mechanisms underlying spontaneous oscillation and rhythmic firing in rat subthalamic neurons. *J Neurosci* **19**:7617–7628.

Breit S, Bouali-Benazzouz R, Popa RC, Gasser T, Benabid AL, and Benazzouz A (2007) Effects of 6-hydroxydopamine-induced severe or partial lesion of the nigrostriatal pathway on the neuronal activity of pallido-subthalamic network in the rat. *Exp Neurol* **205**:36–47.

Brice NL, Varadi A, Ashcroft SJH, and Molnar E (2002) Metabotropic glutamate and $GABA_{(B)}$ receptors contribute to the modulation of glucose-stimulated insulin secretion in pancreatic beta cells. *Diabetologia* **45**:242–252.

Brito GAC, Sachs D, Cunha FQ, Vale ML, Lotufo CMC, Ferreira SH, and Ribeiro RA (2006) Peripheral antinociceptive effect of pertussis toxin: activation of the arginine/NO/cGMP/PKG/ATP-sensitive K channel pathway. *Eur J Neurosci* **24**: 1175–1181.

Canteras NS, Shammah-Lagnado SJ, Silva BA, and Ricardo JA (1990) Afferent connections of the subthalamic nucleus: a combined retrograde and anterograde horseradish peroxidase study in the rat. *Brain Res* **513**:43–59.

Caruso C, Durand D, Watanobe H, and Lasaga M (2006) NMDA and group I metabotropic glutamate receptors activation modulates substance P release from the arcuate nucleus and median eminence. *Neurosci Lett* **393**:60–64.

Chen C-C, Lee S-T, Wu T, Chen C-J, Huang C-C, and Lu C-S (2002) Hemiballism after subthalamotomy in patients with Parkinson's disease: report of 2 cases. *Mov Disord* **17**:1367–1371.

Congar P, Leinekugel X, Ben-Ari Y, and Crépel V (1997) A long-lasting calcium-activated nonselective cationic current is generated by synaptic stimulation or exogenous activation of group I metabotropic glutamate receptors in CA1 pyramidal neurons. *J Neurosci* **17**:5366–5379.

Dunn-Meynell AA, Rawson NE, and Levin BE (1998) Distribution and phenotype of neurons containing the ATP-sensitive K^+ channel in rat brain. *Brain Res* **814**: 41–54.

Ehrlich BE, Kaftan E, Bezprozvannaya S, and Bezprozvanny I (1994) The pharmacology of intracellular $Ca^{(2+)}$-release channels. *Trends Pharmacol Sci* **15**:145–149.

Fagni L, Chavis P, Ango F, and Bockaert J (2000) Complex interactions between mGluRs, intracellular Ca^{2+} stores and ion channels in neurons. *Trends Neurosci* **23**:80–88.

Féger J, Hassani O-K, and Mouroux M (1997) The subthalamic nucleus and its connections. New electrophysiological and pharmacological data. *Adv Neurol* **74**: 31–43.

Fiorillo CD and Williams JT (1998) Glutamate mediates an inhibitory postsynaptic potential in dopamine neurons. *Nature* **394**:78–82.

Guridi J, Herrero MT, Luquin MR, Guillén J, Ruberg M, Laguna J, Vila M, Javoy-Agid F, Agid Y, and Hirsch E, et al. (1996) Subthalamotomy in parkinsonian monkeys. Behavioural and biochemical analysis. *Brain* **119**:1717–1727.

Han J, Kim N, Kim E, Ho W-K, and Earm YE (2001) Modulation of ATP-sensitive potassium channels by cGMP-dependent protein kinase in rabbit ventricular myocytes. *J Biol Chem* **276**:22140–22147.

Henzi V and MacDermott AB (1992) Characteristics and function of Ca^{2+}- and inositol 1,4,5-triphosphate-releasable stores of Ca^{2+} in neurons. *Neuroscience* **46**: 251–273.

Karschin C, Ecke C, Ashcroft FM, and Karschin A (1997) Overlapping distribution of K(ATP) channel-forming Kir6.2 subunit and the sulfonylurea receptor SUR1 in rodent brain. *FEBS Lett* **401**:59–64.

Kass JI and Mintz IM (2006) Silent plateau potentials, rhythmic bursts, and pacemaker firing: three patterns of activity that coexist in quadristable subthalamic neurons. *Proc Natl Acad Sci USA* **103**:183–188.

Kawano T, Zoga V, Kimura M, Liang M-Y, Wu H-E, Gemes G, McCallum JB, Kwok W-M, Hogan QH, and Sarantopoulos CD (2009) Nitric oxide activates ATP-sensitive potassium channels in mammalian sensory neurons: action by direct S-nitrosylation. *Mol Pain* **5**:1–20.

Kuwajima M, Dehoff MH, Furuichi T, Worley PF, Hall RA, and Smith Y (2007) Localization and expression of group I metabotropic glutamate receptors in the mouse striatum, globus pallidus, and subthalamic nucleus: regulatory effects of MPTP treatment and constitutive Homer deletion. *J Neurosci* **27**:6249–6260.

Kuwajima M, Hall RA, Aiba A, and Smith Y (2004) Subcellular and subsynaptic localization of group I metabotropic glutamate receptors in the monkey subthalamic nucleus. *J Comp Neurol* **474**:589–602.

Liss B, Bruns R, and Roeper J (1999) Alternative sulfonylurea receptor expression defines metabolic sensitivity of K-ATP channels in dopaminergic midbrain neurons. *EMBO J* **18**:833–846.

Liss B, Haeckel O, Wildmann J, Miki T, Seino S, and Roeper J (2005) K-ATP channels promote the differential degeneration of dopaminergic midbrain neurons. *Nat Neurosci* **8**:1742–1751.

Maltête D, Jodoin N, Karachi C, Houeto JL, Navarro S, Cornu P, Agid Y, and Welter ML (2007) Subthalamic stimulation and neuronal activity in the substantia nigra in Parkinson's disease. *J Neurophysiol* **97**:4017–4022.

Marino MJ, Awad-Granko H, Ciombor KJ, and Conn PJ (2002) Haloperidol-induced alteration in the physiological actions of group I mGlus in the subthalamic nucleus and the substantia nigra pars reticulata. *Neuropharmacology* **43**:147–159.

Marino MJ and Conn PJ (2006) Glutamate-based therapeutic approaches: allosteric modulators of metabotropic glutamate receptors. *Curr Opin Pharmacol* **6**:98–102.

Mehta A, Menalled L, and Chesselet M-F (2005) Behavioral responses to injections of muscimol into the subthalamic nucleus: temporal changes after nigrostriatal lesions. *Neuroscience* **131**:769–778.

Messenger MJ, Dawson LG, and Duty S (2002) Changes in metabotropic glutamate receptor 1-8 gene expression in the rodent basal ganglia motor loop following lesion of the nigrostriatal tract. *Neuropharmacology* **43**:261–271.

Mironov SL and Richter DW (2000) Intracellular signalling pathways modulate K (ATP) channels in inspiratory brainstem neurones and their hypoxic activation: involvement of metabotropic receptors, G-proteins and cytoskeleton. *Brain Res* **853**:60–67.

Mourre C, Widmann C, and Lazdunski M (1990) Sulfonylurea binding sites associated with ATP-regulated K^+ channels in the central nervous system: autoradiographic analysis of their distribution and ontogenesis, and of their localization in mutant mice cerebellum. *Brain Res* **519**:29–43.

Nunemaker CS, DeFazio RA, and Moenter SM (2003) A targeted extracellular approach for recording long-term firing patterns of excitable cells: a practical guide. *Biol Proced Online* **5**:53–62.

Otsuka T, Murakami F, and Song W-J (2001) Excitatory postsynaptic potentials trigger a plateau potential in rat subthalamic neurons at hyperpolarized states. *J Neurophysiol* **86**:1816–1825.

Rainnie DG, Holmes KH, and Shinnick-Gallagher P (1994) Activation of postsynaptic metabotropic glutamate receptors by trans-ACPD hyperpolarizes neurons of the basolateral amygdala. *J Neurosci* **14**:7208–7220.

Sergeeva OA, Doreulee N, Chepkova AN, Kazmierczak T, and Haas HL (2007) Long-term depression of cortico-striatal synaptic transmission by DHPG depends on endocannabinoid release and nitric oxide synthesis. *Eur J Neurosci* **26**: 1889–1894.

Sharifullina E, Ostroumov K, and Nistri A (2005) Metabotropic glutamate receptor activity induces a novel oscillatory pattern in neonatal rat hypoglossal motoneurones. *J Physiol* **563**:139–159.

Shen K-Z and Johnson SW (2000) Presynaptic dopamine D_2 and muscarine M_3 receptors inhibit excitatory and inhibitory transmission to rat subthalamic neurones *in vitro*. *J Physiol* **525**:331–341.

Shen K-Z and Johnson SW (2010) Ca^{2+} influx through NMDA-gated channels activates ATP-sensitive K^+ currents through a nitric oxide-cGMP pathway in subthalamic neurons. *J Neurosci* **30**:1882–1893.

Shen K-Z and Johnson SW (2012) Chronic dopamine depletion augments the functional expression of K-ATP channels in the rat subthalamic nucleus. *Neurosci Lett* **531**:104–108.

Shinbo A and Iijima T (1997) Potentiation by nitric oxide of the ATP-sensitive K^+ current induced by K^+ channel openers in guinea-pig ventricular cells. *Br J Pharmacol* **120**:1568–1574.

Suzuki M, Muraki K, Imaizumi Y, and Watanabe M (1992) Cyclopiazonic acid, an inhibitor of the sarcoplasmic reticulum Ca(2+)-pump, reduces Ca(2+)-dependent K+ currents in guinea-pig smooth muscle cells. *Br J Pharmacol* **107**:134–140.

Tempia F, Alojado ME, Strata P, and Knöpfel T (2001) Characterization of the $mGluR_{(1)}$-mediated electrical and calcium signaling in Purkinje cells of mouse cerebellar slices. *J Neurophysiol* **86**:1389–1397.

Thastrup O, Cullen PJ, Drøbak BK, Hanley MR, and Dawson AP (1990) Thapsigargin, a tumor promoter, discharges intracellular Ca2+ stores by specific inhibition of the endoplasmic reticulum Ca2(+)-ATPase. *Proc Natl Acad Sci USA* **87**: 2466–2470.

Wang S, Hu LF, Yang Y, Ding JH, and Hu G (2005) Studies of ATP-sensitive potassium channels on 6-hydroxydopamine and haloperidol rat models of Parkinson's disease: implications for treating Parkinson's disease? *Neuropharmacology* **48**: 984–992.

Wang X-S, Ong W-Y, Lee HK, and Huganir RL (2000) A light and electron microscopic study of glutamate receptors in the monkey subthalamic nucleus. *J Neurocytol* **29**:743–754.

Xia Y and Haddad GG (1991) Major differences in CNS sulfonylurea receptor distribution between the rat (newborn, adult) and turtle. *J Comp Neurol* **314**:278–289.

Xu W, Russo GS, Hashimoto T, Zhang J, and Vitek JL (2008) Subthalamic nucleus stimulation modulates thalamic neuronal activity. *J Neurosci* **28**:11916–11924.

Address correspondence to: Steven W. Johnson, Portland VA Medical Center, RD-61, 3710 SW US Veterans Hospital Road, Portland, OR 97207. E-mail: johnsost@ohsu.edu